Applied Radiation and Isotopes 105 (2015) 176–181

Contents lists available at ScienceDirect

Applied Radiation and Isotopes

journal homepage: www.elsevier.com/locate/apradiso

Thermoluminescence dosimetry features of DY and Cu doped SrF_2 nanoparticles under gamma irradiation

M. Zahedifar [a,b,*], E. Sadeghi [a,b], M. Kashefi biroon [a], S. Harooni [a], F. Almasifard [a]

[a] Physics Department, University of Kashan, Kashan, Islamic Republic of Iran
[b] Institute of Nanoscience and Nanotechnology, University of Kashan, Kashan, Islamic Republic of Iran

HIGHLIGHTS

- The SrF_2:Dy and SrF_2:Cu nanoparticles were synthesized for the first time.
- The co-precipitation method as an easy and low cost method was used.
- A linear dose response in a broad range of the absorbed dose was achieved.
- The TL response remains almost unchanged after several cycles of irradiation, annealing and readout.

ARTICLE INFO

Article history:
Received 26 May 2015
Received in revised form
11 August 2015
Accepted 17 August 2015
Available online 19 August 2015

Keywords:
Thermoluminescence
SrF_2:Dy
SrF_2:Cu
Nanoparticles
Radiation dosimetry

ABSTRACT

Dy and Cu-doped SrF_2 nanoparticles (NPs) were synthesized by using co-precipitation method and their possible application to solid state dosimetry were studied and compared to that of pure SrF_2 NPs. X-ray diffraction (XRD), scanning electron microscopy (SEM) and energy dispersive spectrometer (EDS) were used for sample characterization. The highest thermoluminescence (TL) response of SrF_2:Dy and SrF_2:Cu NPs were found respectively at 0.5 and 0.7 mol% of Dy and Cu impurities. Seven overlapping glow peaks at 384, 406, 421, 449, 569, 495, 508 K and three component glow peaks at 381, 421 and 467 K were identified respectively for SrF_2:Dy and SrF_2:Cu NPs employing T_m–T_{stop} and computerized glow curve deconvolution (CGCD) methods. The TL sensitivity of SrF_2:Dy is approximately the same as that of LiF:Mg, Ti (TLD-100) cheeps. Linear dose response were observed for the SrF_2:Dy and SrF_2:Cu NPs up to the absorbed doses of 1 kGy and 10 kGy correspondingly. Regarding other dosimetry characteristics of the produced NPs such as fading, reproducibility and thermal treatment, Dy and Cu doped SrF_2 NPs recommend for high dose TL dosimetry applications.

1. Introduction

The micro-scale alkaline earth fluorides have been amongst the most popular TL dosimeters (McKeever, 1985; Chen, 1984, Vol. 1, Chapter 4). The luminescence of fluorides is connected mainly to the presence of rare earth ions in them (Radzhabov, 2002). Strontium fluoride (SrF2) is one of the most widely used alkaline earth materials because of its interesting luminescent, optical, and physical properties. It has a wide band gap, low phonon energy, low refraction index, high radiation resistance, and good mechanical strength (Ivanovskikh et al., 2005; Van der Ende et al., 2009). Optical properties and irradiation effects in micro-scale Nd^{3+}, Pr^{3+}, Tb^{3+} and Tm^{3+} doped SrF_2 crystals and their possible application to solid-state dosimetry have been studied and compared to those induced in pure SrF_2 crystals (Kristianpoller et al., 2004). However, the TL characteristics of SrF_2 under gamma irradiation have not adequately been studied, especially compared to other alkaline earth fluorides.

In recent years, nanomaterials because of their exceptional TL properties compared with their bulk equivalents, have attracted much attention (Zahedifar et al., 2011; Salah, 2011; Vij et al., 2010). Special optical properties of nano-scaled materials can be explained based on quantum size effect and large surface to volume ratio. Studies on different luminescent nanomaterials have revealed their excellent features such as simple TL glow curve structure and linear TL dose response over wider range of absorbed dose compared with those of corresponding microcrystalline samples. These behaviors have been explained using the track interaction model (Horowitz et al., 2001). Therefore, investigating

* Corresponding author at: Physics Department, University of Kashan, Kashan, Islamic Republic of Iran. Fax: +98 31 55912570.
E-mail address: zhdfr@kashanu.ac.ir (M. Zahedifar).

http://dx.doi.org/10.1016/j.apradiso.2015.08.022
0969-8043/

the TL features of nanostructured counterparts of rare earth doped alkaline earth fluorides would be of importance for their potential application to estimate high doses of ionizing radiations, where the conventional microcrystalline phosphors have a limitation.

In this work, the synthesis procedure, TL kinetic parameters and dosimetry features of SrF_2:Dy and SrF_2:Cu NPs produced by using co-precipitation method are presented and discussed.

2. Experimental procedure

The SrF_2:M (M=Dy, Cu) NPs were prepared from strontium nitrate ($Sr(NO3)_2$, 99.99% purity), ammonium fluoride (NH_4F, 99.99% purity), Brij 35 (99.9% purity), dysprosium nitrate (Dy $(NO_3)_3$ of 99.99% purity) and copper nitrate (Cu $(No_3)_2$ of 99.99% purity), distilled de-ionized water and acetone (Merck Chemical). Firstly, 20 cc solution A and 20 cc solution B were prepared respectively by dissolving 0.500 gr strontium nitrate and 0.500 gr Brij in a mixture of aceton and deionized water. The 20 cc ammonium fluoride solution was prepared by dissolving 0.175 gr NH_4F in a mixture of acetone/water (solution C). Equal volumes of aceton and deionized water were used in the above solutions. The Solution B was added slowly to solution A while was placed on a stirrer and different amounts of dysprosium nitrate (copper nitrate) was added to it and finally solution C was added slowly while stirred. Lastly, the precipitate was centrifuged, washed with the mixture of acetone/water for several times. The final SrF_2:Dy (SrF2:Cu) NPs were obtained following drying the product in an oven at 90 °C and atmosphere pressure for 3 h.

3. Characterization

Powder X-ray diffraction patterns of the samples were recorded using an X-ray diffractometer (Bruker D8 Advance) with Cu K_α radiation (λ=1.54 Å) under the conditions of 40 kV and 30 mA, at a step size of 2θ=0.02°. SEM images were obtained using a scanning electron microscope model Philips XL-30 ESEM equipped with energy dispersive spectrometer (EDS).

The powder samples were placed in a Teflon container and the electron equilibrium condition was fulfilled in irradiation process. Dose of ionizing radiation were administrated to the powder samples with a ^{60}Co gamma source at the secondary standard dosimetry laboratory (SSDL) facilities, Karaj, Iran. The TL readouts were taken in a Harshaw model 4500 computer-based TL reader using a contact heating where the temperature of the heater strip (planchet) is recorded as indicator of the temperature of the sample with a precision of 1 °C. All TL readouts (apart from readouts in studying the fading characteristic), were carried out 3 hours after irradiation to allow tunneling and transitions between trapping states. The heating rate for readout was 1 °C/s (with preheat of 50 °C) to a maximum temperature of 350 °C. The samples were annealed at 400 °C for 15 min using a programmable oven with temperature precision of 1 °C and then were cooled rapidly to room temperature (75 °C/min). All the experiments were carried out using the samples produced in a single synthesis procedure. The TL responses of the samples of different batches under the same irradiation conditions were the same through an uncertainty of 5%. Since the TL response depends on the mass of the sample, it was kept constant at 0.005 gr using Sartorius Research. R 160 P weigher (with a mass accuracy of ± 0.01 mg).

4. Results and discussion

Fig. 1(a–c) shows the X-ray diffraction patterns of the synthesized SrF_2:Dy (a), SrF_2:Cu (b) and pure SrF_2 (c) NPs. Except for very low differences in the peak intensities due to different impurities, the patterns are the same which confirm that the sample is SrF_2 with cubic structure and corresponds to JCPDS card no. 86-2418. From XRD results, the average particle size was calculated by Scherrer's formula from which the crystalline size of approximately 21 nm obtained using the dominant (111) peak. This result is in agreement with the SEM image of Fig. 2. Fig. 2(a and b) shows respectively the SEM images of SrF_2:Dy and SrF_2:Cu NPs. As is evident in this figure, the NPs have approximately the same size and spherical shape. EDS spectrum is observed in Fig. 3(a and b) which reveal that the products are SrF_2: Dy (a) and SrF_2: Cu (b) without contamination. The elemental concentrations are shown in the insets of Fig.3.

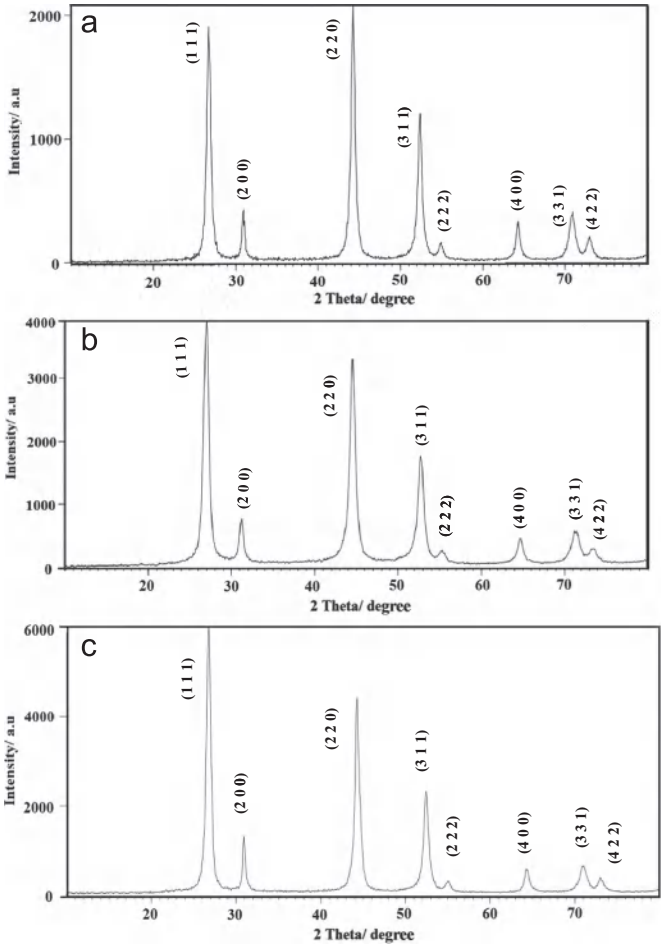

Fig. 1. (a–c). X-ray diffraction pattern of the synthesized SrF_2:Dy (a), SrF_2:Cu (b) and pure SrF_2 (c) NPs. Except for very low differences in peak intensities, the XRD patterns are the same, indicating that the host crystal is SrF_2.

The $T_m - T_{stop}$ method was employed to identify the number of component glow peaks contained in the complex glow curve of the synthesized NPs. Using this method, firstly a pre-readout anneal up to T_{stop}, in the temperature range of 90–220 °C was applied to bleach the low temperature portion of the glow curve, followed by cooling the sample to room temperature and readout for recording the TL glow curve (Zahedifar et al., 2013). Fig. 4(a and b) shows respectively the variation of T_m versus T_{stop} for the glow curves of SrF_2:Dy and SrF_2:Cu NPs subsequent to administrated dose of 100 Gy by ^{60}Co gamma source. All the samples were first annealed to a specific temperature, T_{stop} with a constant heating rate of 5 °C/s, then cooled rapidly to room temperature in nitrogen atmosphere followed by readout with a heating rate of 2 °C/s for

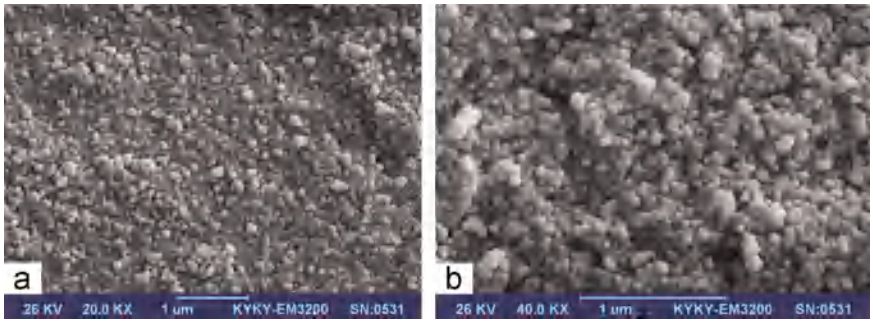

Fig. 2. SEM images of the produced SrF_2:Dy (a) and SrF_2:Cu (b) NPs.

recording the glow curve. As is evident, by increasing the T_{stop}, the T_m moves towards higher temperatures, but this variation is not monotonic and several jumps are observed in T_m values. The temperature region in which T_m does not change abruptly belongs to a specific glow peak. Increase in T_m with T_{stop} in a specific temperature region, can be attributed to overlapping glow peaks in that region. Four plateaus and three distinct jumps are observed in T_m–T_{stop} pattern of SrF_2:Dy NPs (Fig. 4(a)). In the first and the last plateaus, the T_m remains almost constant which shows that each plateau region attributes to a single glow peak. The T_m in the two middle plateaus increases monotonically with T_{stop} indicating that two or more overlapping component glow peaks are there in each temperature region of these middle plateaus. The T_m–T_{stop} curve of SrF_2Cu NPs includes three plateaus and two definite jumps, an indication of three component glow peaks. Therefore, the minimum number of 6 component glow peaks for SrF_2:Dy and three components for SrF_2Cu NPs were considered as input parameter for the computerized glow curve deconvolution (CGCD) procedure.

This program which has been produced in our laboratory using the Levenberg–Marquart algorithm based on non-linear least square method, uses general order of kinetics, mixed order of kinetics and complex functions describing continuous trap distribution to obtain the kinetic parameters of the deconvoluted glow peaks (Levenberg, 1944). TL General order glow curve deconvolution function was used to obtain the kinetic parameters of the component glow peaks (Kitis et al.,1998).

The used glow curve deconvolution function (in terms of I_m, T_m, E and b) has advantage over the deconvolution function in terms of n_o (initial concentration of electrons in trapping states), s (the pre exponential factor), E and b since I_m and T_m can easily be estimated from the experimental glow curve as the initial values for curve fitting procedure. Also the used function for general order of kinetics is more useful than the deconvolution functions for limiting cases of first and second-orders of kinetics because intermediate cases in which $1 < b < 2$ can be dealt with and it smoothly goes to first and second orders when $b \to 1$ and $b \to 2$, respectively (Bos, 2007). For testing the goodness of fit, the figure of merit (FOM) was used (Balian and Eddy, 1977):

$$\mathrm{FOM} = \sum_{j_i}^{j_f} \frac{100|y_i - y(x_i)|}{A} \tag{1}$$

where j_i and j_f are the numbers of the first and last temperature interval ΔT used for curve fitting, y_i is the intensity in the ith interval obtained from experiment and $y(x_i)$ the intensity expected from theory and A, the total area of the fitted glow peak between j_i and j_f. The FOM values lower than 2.5% shows good fitness to the experimental glow curves. The result of CGCD procedure applied to SrF_2:Dy and SrF_2:Cu NPs for administrated doses of 500 Gy and 100 Gy are shown respectively in Fig.5(a and b). Considering 7 glow peak components for TL glow curve of SrF_2:Dy NPs as an input in CGCD process resulted in minimum value of 0.75% for the FOM in Fig. 5(a), which shows superior fitness of experimental and the theoretical glow peaks. As an output of CGCD procedure, the seven overlapping glow peaks are observed in this figure at 384, 406, 421, 449, 569, 495 and 508 K. The outcome of CGCD for SrF_2:Cu NPs is seen in Fig.5(b). Three well-separated component glow peaks are located at 381, 421 and 467 K. The low FOM value of 0.86% shows an excellent fitness of the experimental glow curve with that generated by the program. In addition, the activation energy, kinetic order and peak temperature of the constructing glow peaks of SrF_2:Dy and SrF_2:Cu NPs are presented in Table 1(a and b).

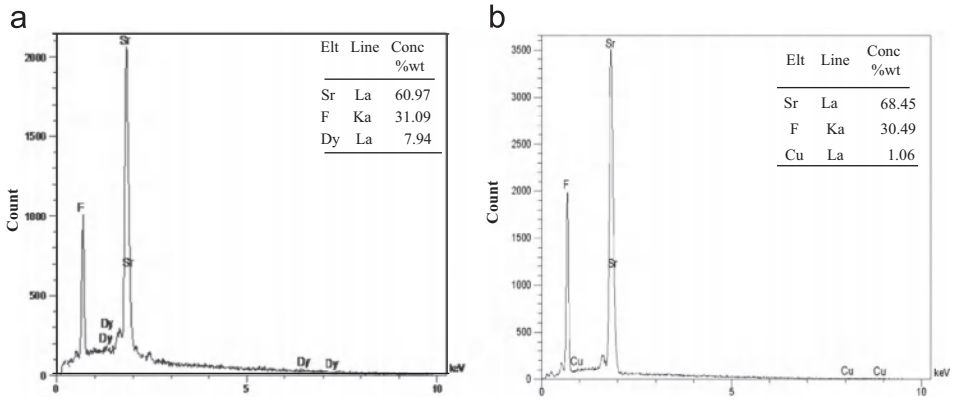

Fig. 3. EDS spectra of synthesized SrF_2:Dy (a) and SrF_2:Cu (b) NPs. The concentration of different elements is shown in the inset of the figure.

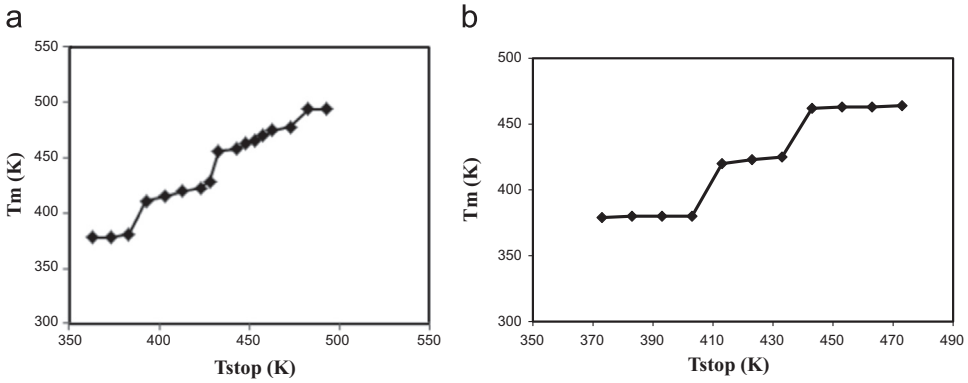

Fig. 4. Variation of peak maximum (T_m) versus T_{stop} for SrF_2:Dy (a) and SrF_2:Cu (b) NPs.

The TL sensitivity is highly depends on the kind and amount of impurity ion. So the effect of concentration of Dy and Cu on TL sensitivity of SrF_2:Dy and SrF_2:Cu nanoparticles was taken into account. The TL responses of the synthesized NPs with various Dy^{3+} and Cu^{2+} concentrations for administrated γ-ray dose of 100 Gy are depicted in Fig.6(a and b). It is observed in Fig. 6(a) that the area underneath the TL glow curve increases with increasing dysprosium concentration from 0.1 mol% to 0.5% while at higher Dy concentrations, the glow curve area falls rapidly. Therefore, the optimum concentration of Dy^{3+} was found at 0.5 mol%. The most favorable amount of Cu impurity in SrF_2:Cu NPs is 0.7 mol% as is apparent in Fig.6(b). A comparison of TL glow curves of the produced SrF_2:Dy and SrF_2:Cu NPs with the commercial LiF:Mg,Ti (TLD-100) after irradiating the samples to the same dose of 1 Gy by ^{60}Co source and correcting the responses for masses of the samples is presented in Fig.7. In addition, it was found that the shapes of TL glow curves of pure SrF_2 NPs and Cu doped SrF_2 NPs are approximately the same and the only difference is the higher TL sensitivity of Cu doped SrF_2 NPs which justifies that the Cu ion plays mainly as an activator in TL process in SrF_2 NPs.

Linear TL dose response is an important parameter essential for any TL material that is used for dosimetry applications. For studying the linearity of dose response, samples of SrF_2:Dy and SrF_2:Cu NPs of the same masses were exposed to different doses by ^{60}Co source and the TL responses were recorded for different absorbed doses. The results are shown in Fig. 8(a and b) for SrF_2:Dy and SrF_2:Cu NPs correspondingly in a log–log scale. Considering relatively high fading of two lower temperature glow peaks in both SrF_2:Dy and SrF_2:Cu NPs as will be discussed in this section, it is constructive to obtain the dose response curves in absence of these glow peaks. Therefore, the samples were firstly heated by a constant rate of 5 °C/s up to the temperature sufficient for detrapping two lower temperature glow peaks and in subsequent heating the sample, the total glow curve area was recorded as dose response. In Fig. 8(a and b), plot 1 shows the dose response of samples including glow peaks 1, 2, while plot 2 represents the dose response in which the areas of glow peaks 1, 2 have been eliminated from the total curve area. As is obvious in

Table 1
TL kinetic parameters of the component glow peaks of the synthesized SrF_2:Dy (a) and SrF_2:Cu (b) NPs, obtained by the CGCD method for the received dose of 500 Gy (a) and 100 Gy (b).

Peak	b	E (eV)	T_m (K)	I_m (a.u)
(a)				
1	1.35	1.21	384	24630
2	1.02	1.42	406	4384
3	1.89	1.36	421	11934
4	1.01	1.10	449	893
5	1.98	1.38	469	6938
6	1.00	2.03	495	1248
7	1.42	1.98	508	2563
(b)				
1	1.11	1.19	381	1702
2	1.11	1.20	421	635
3	1.49	1.53	467	438

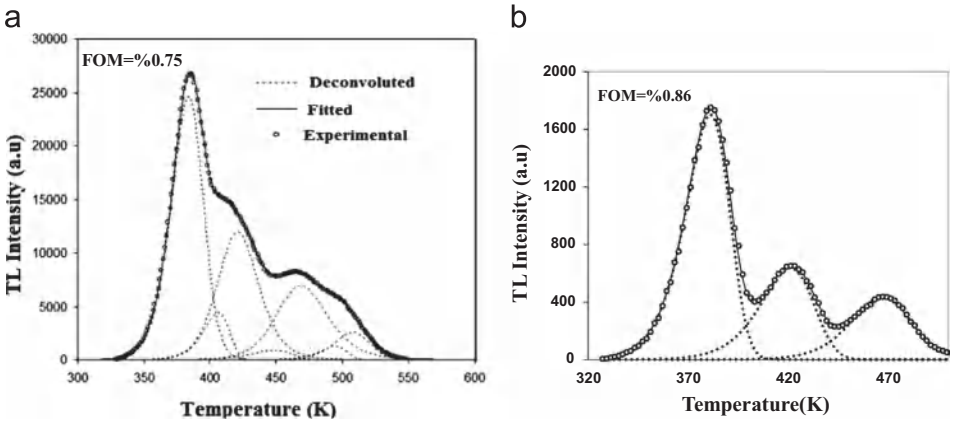

Fig. 5. Experimental TL glow curve (hollow circles), fitted glow curve (solid curve) along with component glow peaks (dashed curves) for the SrF_2:Dy (a) and SrF_2:Cu(b) NPs for absorbed dose of 500 Gy (a) and 100 Gy (b).

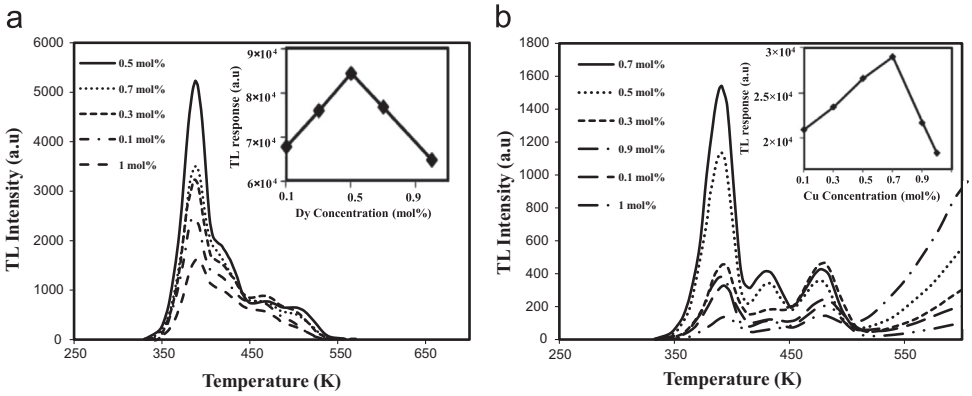

Fig. 6. The TL glow curves of SrF_2 NPs doped with different concentrations of Dy (a) and Cu (b) following administrated dose of 100 Gy. The corresponding plots which show the variation of TL responses versus the impurity concentrations for the same absorbed dose of 100 Gy are shown as the insets of the figure.

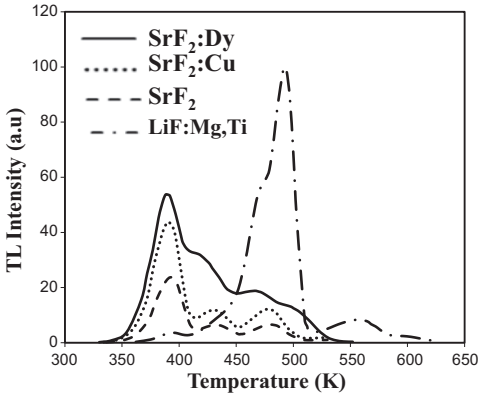

Fig. 7. Comparison of the TL glow curves of the pure SrF_2, SrF_2:Dy, SrF_2:Cu NPs and LiF:Mg,Ti (TLD-100) for the absorbed dose of 1 Gy from ^{60}Co gamma source. TL glow curves of pure SrF_2 and SrF_2:Cu NPs were enlarged by a factor of 2 for better presentation.

this figure, while the TL dose response of SrF_2:Dy is linear up to absorbed dose of 1000 Gy, an approximately linear dose response up to 10kGy is observed for SrF_2:Cu NPs. In order to determine the thermal fading of the synthesized SrF_2:Dy and SrF_2:Cu NPs, samples were irradiated to the same dose of 100 Gy and were kept out in dark place at room temperature. The TL signals of the irradiated samples were recorded for different storage times up to 30 days. The results are shown in Fig. 9(a and b). It is seen in Fig.9(a) that whilst the low temperature TL glow peak of SrF_2:Dy NPs disappears after storing the samples for two weeks, only a small reduction in TL signal of higher temperature peaks are observed after 30 days. Also, the fading of TL glow curve of SrF_2:Cu NPs shown in Fig.9(b), demonstrates that the glow peak 1 disappears after 2 weeks at room temperature. Fig.10(a) shows that the area underneath the TL glow curve of SrF_2:Dy NPs not including peak 1 and not including peaks 1+ 2 decreases respectively to 15% and 5% of its original value following a storage time of 1 month. The reduction in TL signal of SrF_2:Cu NPs without peak 1 and without peaks 1+2 are 20% and 16% correspondingly (Fig.10(b)). The reusability without reduction in TL response is a main feature for each TL dosimeter. In this study, the reusability of this nanophosphor was also studied. To do so, the TL responses of seven samples having the same masses were recorded after 6 successive cycles of annealing, irradiation and readout following an administrated dose of 50 Gy. The average TL responses and the standard deviations for 6 cycles are shown in Fig. 11. According to this figure, the TL responses remain approximately unchanged after 6 above mentioned cycles.

5. Conclusions

The synthesized SrF_2:Dy and SrF_2:Cu NPs exposed to different dose levels showed a promising TL characteristic. They have good sensitivity for high levels of absorbed dose. Their linear dose response over a large span of exposure make them good candidates for high dose dosimetry applications. The outstanding dosimetry feature of the synthesized SrF_2:Dy is that while its TL sensitivity is comparable with the commercial LiF:Mg,Ti TL dosimeter, at the same time its dose responses is linear beyond the high absorbed dose of 1000 Gy. The study of TL dosimetry features of the above NPs under high LET radiation is also suggested.

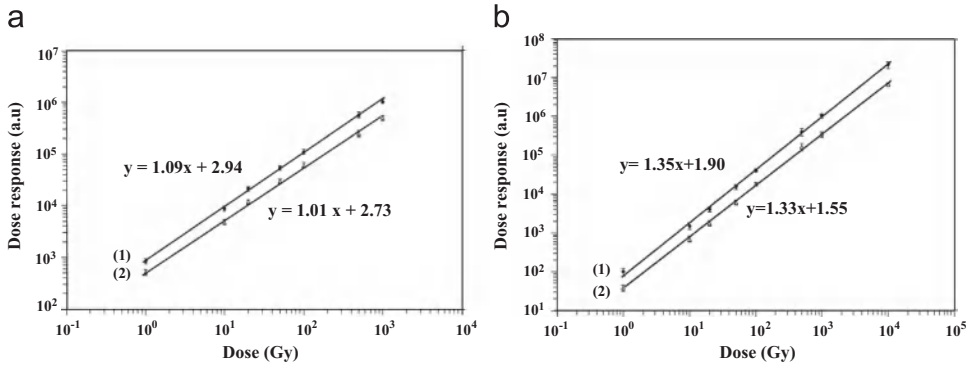

Fig. 8. Dose response plots of SrF_2:Dy (a) and SrF_2:Cu (b) NPs in log–log scale. The slopes near one, show that the responses are linear in the observed range of absorbed doses. The intercepts in both plots (a and b) give the logarithm of the count per unit dose. The Plots 1 and 2 show the dose response in presence and absence of two lower temperature glow peaks respectively.

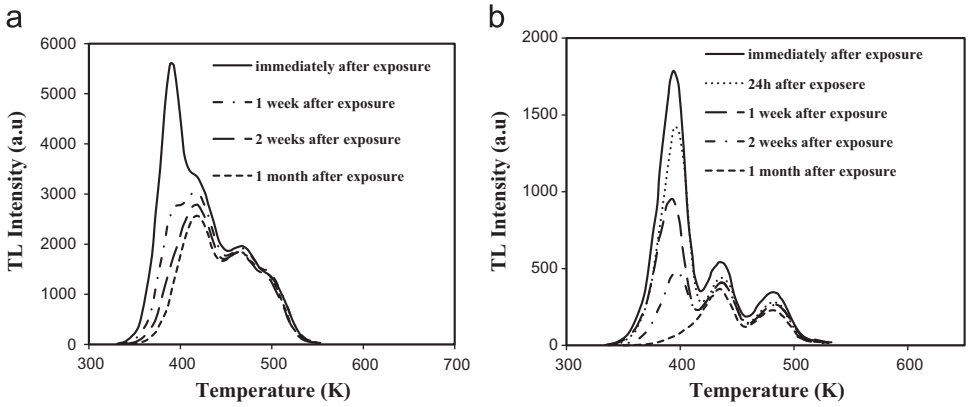

Fig. 9. Decrease in TL glow curve area of the synthesized SrF_2:Dy (a) and SrF_2:Cu (b) NPs by storage time. The samples were first irradiated to the same dose of 100 Gy by ^{60}Co source.

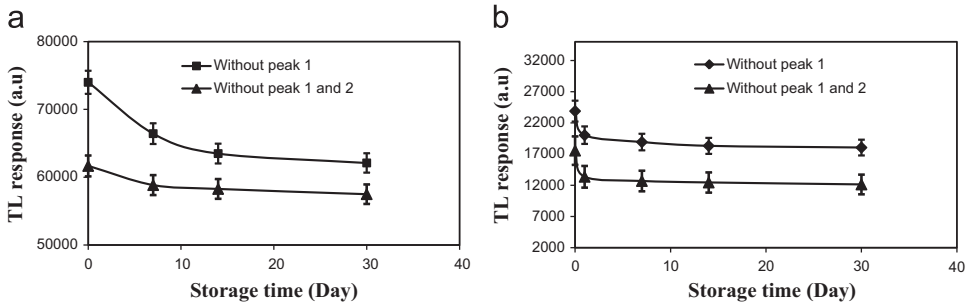

Fig. 10. Fading characteristic of TL signal of SrF_2:Dy (a) and SrF_2:Cu (b) NPs at room temperature (a) without peak 1 and (b) without peaks 1 + 2 after received dose of 100 Gy.

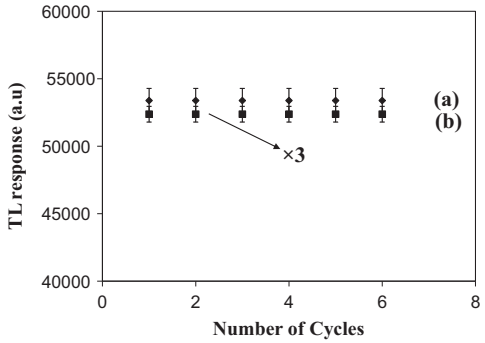

Fig.11. TL responses of SrF_2:Dy (a) and SrF_2:Cu (b) NPs for 6 successive cycles of annealing, irradiation to the same dose of 50 Gy and readout. The TL response of SrF_2:Cu (b) was enlarged by a factor of 3 for comparison purposes.

Acknowledgements

The research council of the University of Kashan is gratefully acknowledged for the financial support of this work.

References

Balian, H.G., Eddy, N.W., 1977. Figure of merit (FOM), an improved criterion over the normalized chi squared test for assessing goodness-of-fit of gamma-ray spectra peaks. Nucl. Instrum. Methods 145, 389–393.

Bos., A.J.J., 2007. Theory of thermoluminescence. Radiat. Meas. 41, 45–56.

Chen, R., 1984. Thermoluminescence and Thermoluminescent Dosimetry. In: Horowitz, Y.S. (Ed.), 1984. CRC Press, Boca Raton.

Horowitz, Y.S., Avila, O., Rodriguez-Villafuerte, M., 2001. Nucl. Instrum. Methods B 184, 85.

Ivanovskikh, K.V., Pustovarov, V.A., Krim, M., Shulgin, B.V., 2005. Time-resolved vacuum ultraviolet spectroscopy of Er^{3+} ions in the SrF_2 crystal. J. Appl. Spectrosc. 72, 564–568.

Kitis, G.G., Gomez Ros, J.M., Tuyn, J.W.N., 1998. Thermoluminescence glow curve deconvolution functions for first, second and general orders of kinetics. J. Phys. D:Appl. Phys. 31, 2636–2641.

Kristianpoller, N., Weiss, D., Chen, R., 2004. Optical and dosimetric properties of variously doped SrF_2 crystals. Radiat. Meas. 38, 719–722.

Levenberg, K., 1944. A method for the solution of certain non-linear problems in least squares. Q. Appl. Math. 2, 164–168.

McKeever, S.W.S., 1985. Thermoluminescence of Solids. Cambridge University Press, Cambridge.

Salah, N., 2011. Nanocrystalline materials for the dosimetry of heavy charged particles: a review. Radiat. Phys. Chem. 80, 1–10.

Vij, A., Lochab, S.P., Kumar, R., Singh., N., 2010. Thermoluminescence response and trap parameters determination of gamma exposed Ce doped SrS nanostructures. J. Alloys Compd. 490, L33–L36.

Zahedifar, M., Mehrabi, M., Harooni, S., 2011. Synthesis of $CaSO_4$: Mn nanosheets with high thermoluminescence sensitivity. Appl. Radiat. Isot. 69, 1002–1006.

Van der Ende, B.M., Aarts, L., Meijerink, A., 2009. Near-infrared quantum cutting for photovoltaics. Adv. Mater. 21, 3073–3077.

Zahedifar, M., Sadeghi, E., Mozdianfard, M.R., Habibi, E., 2013. Synthesis, characteristics and thermoluminescent dosimetry features of γ-irradiated Cedoped CaF2 nanophosphor. Appl. Radiat. Isot. 78, 125–131.